Mass Spectrometric Investigation of the Mechanism of Inactivation of Hamster Arylamine N-Acetyltransferase 1 by N-Hydroxy-2-Acetylaminofluorene

ARTICLE *in* CHEMICAL RESEARCH IN TOXICOLOGY · APRIL 2004

Impact Factor: 3.53 · DOI: 10.1021/tx030045o · Source: PubMed

3 AUTHORS, INCLUDING:

Carston R Wagner
University of Minnesota Twin Cities
86 PUBLICATIONS **1,544** CITATIONS

SEE PROFILE

Chemical Research in Toxicology

MARCH 2004
VOLUME 17, NUMBER 3

Articles

Mass Spectrometric Investigation of the Mechanism of Inactivation of Hamster Arylamine N-Acetyltransferase 1 by N-Hydroxy-2-Acetylaminofluorene

Zhijun Guo, Carston R. Wagner, and Patrick E. Hanna*

Department of Medicinal Chemistry, University of Minnesota, 308 Harvard Street Southeast, Minneapolis, Minnesota 55455

Received October 6, 2003

Arylamine N-acetyltransferases (NATs) are expressed in most mammalian tissues. NATs catalyze the N-acetylation of primary arylamines, the O-acetylation of N-arylhydroxylamines, and the N,O-transacetylation of N-arylhydroxamic acids. The latter two reactions result in formation of reactive, electrophilic N-acetoxyarylamines, which are considered to be the ultimate carcinogenic metabolites of certain environmental and dietary arylamines. Incubation of various N-(aryl)acetohydroxamic acids, such as N-hydroxy-2-acetylaminofluorene (N-OH-AAF) with hamster NAT1, results in time-dependent, concentration-dependent, and kinetically first-order irreversible inactivation of the enzyme. N-OH-AAF also causes in vivo inactivation of NAT1. The purpose of this research was to investigate the molecular mechanism of NAT1 inactivation by identifying the amino acid residues that undergo covalent modification upon NAT1-catalyzed bioactivation of N-OH-AAF and by characterizing the chemical structures of the adducts. Electrospray ionization quadrupole time-of-flight mass spectrometric analysis of NAT1 that had been incubated with N-OH-AAF revealed that the mass of the major adduct (+195 Da) was consistent with a (2-fluorenyl)sulfinamide modification. The major adduct underwent hydrolysis to yield a protein with a molecular mass that corresponded to a sulfinic acid-modified NAT1. Treatment of NAT1 with 2-nitrosofluorene resulted in a modification (+195 Da) that was identical in mass to that obtained with N-OH-AAF-inactivated enzyme. Matrix-assisted laser desorption−ionization quadrupole time-of flight tandem mass spectrometric (MALDI Q-TOF MS/MS) analysis revealed that the modified residue was the catalytically essential Cys68. MALDI Q-TOF MS/MS sequencing of peptides from protease digests of inactivated NAT1 also identified two minor adducts at Tyr17 and Tyr186, each of which was covalently conjugated with 2-aminofluorene. Thus, the mechanism of inactivation of NAT1 by N-OH-AAF involves NAT1-catalyzed deacetylation to afford N-hydroxy-2-aminofluorene, which after oxidative conversion to 2-nitrosofluorene, forms a sulfinamide adduct by reacting with Cys68. GSH had little effect on the inactivation of NAT1 by N-OH-AAF, although high concentrations of cysteine attenuated both the extent of inactivation and the sulfinamide adduct formation.

Introduction

Covalent adduct formation, resulting from the reaction of biotransformation products with nucleophilic sites in cellular DNA, is believed to be requisite for the initiation of tumorigenesis by carcinogenic arylamines and arylamides, such as 2-AF[1] and 2-AAF (*1*, *2*). The conversion of numerous N-aryl carcinogens to electrophilic reactants depends on metabolic N-hydroxylation and subsequent conjugative esterification of the N-hydroxyl group (*3*, *4*).

* To whom correspondence should be addressed. Tel: 612-625-4152. Fax: 612-624-0139. E-mail: hanna002@umn.edu.

10.1021/tx030045o CCC: $27.50
Published on Web 02/18/2004

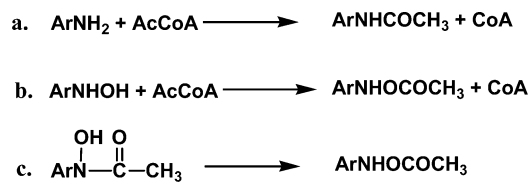

Figure 1. Reactions catalyzed by NATs. (a) N-acetylation of primary arylamines; (b) O-acetylation of N-arylhydroxylamines (OAT activity); and (c) N-arylhydroxamic acid N,O-transacetylation (N,OAT or AHAT activity).

Although certain N-arylhydroxylamines can react directly with DNA, their conversion to N-sulfonyloxy or N-acetoxy esters substantially enhances the rate and extent of adduct formation. N-Arylhydroxamic acids, the product of either arylamide N-hydroxylation or N-arylhydroxylamine N-acetylation, are not electrophilic and require esterification prior to reacting with nucleophilic functional groups in DNA.

Although DNA adducts of numerous arylamines and arylamides have been characterized, much less information is available regarding irreversible adduction of specific proteins by this group of carcinogens. Early reports established that substantial quantities of protein adducts are formed when carcinogenic arylamines and arylamides are administered to laboratory animals (*5*, *6*), and it is apparent that formation of protein−carcinogen adducts can be expected to play a significant role in the physiological disposition of these agents and in the manifestation of their toxicological effects.

NATs (EC 2.3.1.5) are polymorphic enzymes present in cell cytosol and have been identified as having roles in both the detoxification and the bioactivation of arylamine carcinogens (*7*). NATs catalyze the AcCoA-dependent acetylation of arylamines, which is usually considered a detoxification process (Figure 1a), as well as the conjugation of N-arylhydroxylamines by AcCoA-dependent O-acetylation to form electrophilic N-acetoxy esters (Figure 1b). NATs also generate N-acetoxy esters by catalyzing the AcCoA-independent activation of N-arylhydroxamic acids (Figure 1c). As a result of the apparent importance of NATs in detoxification and bioactivation, relationships between NAT polymorphisms, arylamine exposure, and cancer incidence are receiving intense scrutiny (*8*).

We reported that treatment of partially purified hamster or rat NAT preparations with N-arylhydroxamic acids, such as N-OH-AAF, resulted in an irreversible loss of certain NAT activities but not of others (*9*, *10*). The inactivation is the consequence of NAT-catalyzed conversion of N-arylhydroxamic acids to one or more reactive products and appeared to involve a process similar to the cytosolic N-arylhydroxamic acid N,OAT activity (Figure 1c) reported earlier for the metabolic conversion of N-arylhydroxamic acids to electrophilic reactants, which formed arylamine adducts with nucleic acids and methionine (*11*, *12*). Our proposal that N-arylhydroxamic acid-mediated inactivation of NAT was the result of covalent adduct formation between critical NAT residues and electrophilic reactants generated through the N,OAT process (Figure 1c) was supported by the determination of a linear correlation between the extent of loss of NAT activity and the protein adduction of radiolabel from N-OH-AAF (*10*). A variety of structurally related N-arylhydroxamic acids proved to be substrates for the bioactivation/NAT inactivation reaction, and the inactivation rates for most substrates exhibited apparent first-order kinetics (*13*−*16*). The selectivity of the inactivation process was further demonstrated when it was shown that administration of N-OH-AAF to hamsters resulted in loss of hepatic NAT1 activity but had no effect on NAT2 (*17*).

A detailed kinetic analysis of the self-catalyzed inactivation of NATs in the presence of N-OH-AAF was made possible by our development of a protocol for the expression and purification of hamster recombinant NATs (*18*, *19*). N-OH-AAF was shown to be a substantially more efficient inactivator of hamster NAT1 than NAT2, and the characteristics of inactivation of both isozymes fit the general criteria for a mechanism-based process, with the exception that high concentrations of the nucleophilic amino acid, cysteine, protected both NAT1 and NAT2 from the effects of N-OH-AAF (*19*). In the present paper, we describe the use of mass spectrometric analysis to identify the modified amino acids generated during the bioactivation of the carcinogenic N-arylhydroxamic acid, N-OH-AAF, by NAT1 and provide definitive evidence that 2-nitrosofluorene is the biotransformation product that is primarily responsible for inactivation of the enzyme.

Experimental Procedures

Caution: *N-OH-AAF, 2-AF, 2-nitrofluorene, and 2-nitrosofluorene should be handled in accordance with NIH Guidelines for the Laboratory Use of Chemical Carcinogens (20).*

Materials and Methods. N-OH-AAF was synthesized as reported (*21*). DEAE Sepharose Fast Flow anion exchange resin and TPCK-treated trypsin were purchased from Amersham Pharmacia Biotech; pepsin A, endopeptidase Glu-C, and endopeptidase Lys-C were obtained from Sigma. *Escherichia coli* BL-21 Codon Plus RIL cells were purchased from Stratagene. Bio-Spin 6 Tris columns were purchased from Bio-Rad. TFA and formic acid were purchased from Aldrich. The rpHPLC columns 214MS54 and 218MS21 were purchased from Vydac. Other reagents, chemicals, and chromatography materials were obtained from the previously cited sources (*18*, *19*). Protein concentrations were determined with the Bradford assay (*22*). Spectrophotometric data were collected with a Varian Cary 50 UV−vis spectrophotometer. All HPLCs were performed with a Beckman Coulter Gold system equipped with a diode array UV detector. All buffers were degassed under vacuum, and all incubations were conducted under aerobic conditions. Data were analyzed by one way ANOVA with SAS 0.8 software (SAS Institute, Inc., Cary, NC).

Synthesis of 2-Nitrosofluorene. A modification of reported methods was used (*21*, *23*). Pd/C (10%, 100 mg) was added to 2-nitrofluorene (2 mmol, 422 mg) dissolved in anhydrous tetrahydrofuran (100 mL) at 0−2 °C under argon. Hydrazine hydrate (55%, 400 mL) was added slowly to maintain the temperature below 5 °C. The disappearance of 2-nitrofluorene was monitored by TLC (silica gel, ethyl acetate:*n*-hexane, 1:5). After approximately 45 min, the reaction mixture was quickly filtered through Celite and the filtrate was evaporated under vacuum. The residue was dissolved in cold ethyl acetate (100 mL) and was extracted with degassed, cold water (2 × 100 mL). The organic solution was evaporated to dryness under vacuum, and the solid residue was dissolved in cold DMF (80 mL)/

[1] Abbreviations: 2-AAF, 2-acetylaminofluorene; AcCoA, acetyl CoA; 2-AF, 2-aminofluorene; DMSO, dimethyl sulfoxide; ESI, electrospray ionization; EDTA, ethylenediaminetetraacetic acid; EtOH, ethanol; IPTG, isopropyl-*β*-D-thiogalactopyranoside; MALDI, matrix-assisted laser desorption ionization; NAT, arylamine N-acetyltransferase; N,-OAT, N,O-acyltransferase; N-OAc-AF, N-acetoxy-AF; N-OH-AAF, N-hydroxy-AAF; N-OH-AF, N-hydroxy-AF; OAT, O-acetyltransferase; Q-TOF, quadrupole time-of-flight; rpHPLC, reverse phase HPLC; TFA, trifluoroacetic acid.

degassed water (20 mL), which was then added dropwise with vigorous stirring to 0.04 N ferric ammonium sulfate in 0.08 N sulfuric acid (100 mL) at 0 °C. After 10 min, cold degassed water (200 mL) was added; the mixture was filtered to afford a green powder, which was dissolved in chloroform and washed with water. The chloroform solution was evaporated under vacuum, and the resulting green powder was dissolved in *n*-hexane at 40 °C. Cooling the *n*-hexane solution to 0 °C resulted in crystallization of 2-nitrosofluorene, which was collected by filtration and dried under vacuum (300 mg, 75%); mp 80−82 °C (lit mp 77−79 °C); UV (95% EtOH) λ max 362 nm (*23*).

Expression and Purification of Hamster Recombinant NAT1. Expression construct pPH9D has been reported (*19*). Competent BL-21 Codon Plus RIL *E. coli* cells were transformed with pPH9D according to the supplier's instructions. Plasmid-containing colonies were selected on LB/ampicillin (100 μg/mL)/chloramphenicol (50 μg/mL) plates. Overnight cultures (10 mL) were grown from single colonies, and a 1% inoculum was added to 1 L of Terrific Broth containing 100 μg of ampicillin per mL in a 2 L flask. Cultures were grown aerobically with shaking at 250 rpm at 37 °C to an O.D. 600 of 0.3, at which time IPTG was added to a final concentration of 200 μM. After additional incubation for 8 h, the cells were harvested by centrifugation at 5000*g* for 15 min at 4 °C. The cell pellets were quick-frozen in a dry ice−acetone bath and stored at −80 °C. NAT1 was purified as previously described (*19*) with the following modifications: DEAE Sepharose Fast Flow anion exchange resin was used for anion exchange chromatography; the column size was 2.5 cm × 20 cm. The purified enzyme was homogeneous according to SDS−PAGE and ESI Q-TOF MS.

NAT1 Activity Assay. The assay, with N-OH-AAF as the acetyl donor and 4-aminoazobenzene as the acceptor, was carried out at 37 °C as previously described, except that the final concentration of N-OH-AAF was 1.0 mM (*24*).

Sample Preparation for ESI Q-TOF MS of N-OH-AAF-Treated NAT1. To NAT1 (120 μg, 72 μM) in potassium phosphate buffer (49 μL, 20 mM, 1 mM EDTA, 10% glycerol, 0.1 mM DTT, pH 7.4) was added N-OH-AAF dissolved in 1 μL of DMSO. The final concentration of N-OH-AAF was 0.5 mM. DMSO only was added to control incubation mixtures. The mixture was incubated for 1 min at 23 °C, which resulted in loss of activity of greater than 90%. After the incubation, 50 μL of the incubation buffer was added to the reaction mixture to make the final volume 100 μL. The inactivation was then terminated by transferring the reaction mixture to a Bio Spin 6 Tris column, which had been equilibrated with the incubation buffer. After the mixture was centrifuged at 1000*g* for 4 min at 4 °C, 10 μL of the solution was used to assay for protein concentration (*22*) and residual NAT1 activity. To the remaining solution, 20 μL of 10% acetic acid was added slowly, followed by 1 μL of 1% TFA when TFA was the ion-pairing reagent for rpHPLC; 20 μL of 10% formic acid was added instead of acetic acid and TFA, when the ion-pairing reagent was formic acid. The mixture was centrifuged at 16 000*g* for 5 min at 4 °C and was subjected to rpHPLC on a Vydac C4 MS column (214MS54, 4.6 mm × 250 mm). A stepwise isocratic elution with a flow rate of 1 mL/min was used. Solvent A was 5% acetonitrile in either 0.01% TFA or 2% formic acid. Solvent B was 95% acetonitrile in either 0.01% TFA or 2% formic acid. The column was eluted with 100% A (2 min), 35% B (4 min), 65% B (7 min), and 100% B (5 min). The absorbance of the eluate was monitored at 220 and 280 nm. NAT1 eluted at 10.4 min with 0.01% TFA and 10.3 min with 2% formic acid. The protein-containing fractions were stored at −80 °C.

Sample Preparation for ESI Q-TOF MS of 2-Nitrosofluorene-Treated NAT1. To NAT1 (220 μg, 67 μM) in potassium phosphate buffer (98 μL, 20 mM, 1 mM EDTA, 10% glycerol, 0.1 mM DTT, pH 7.4) was added 2-nitrosofluorene dissolved in 2 μL of DMSO. The final concentration of 2-nitrosofluorene was 250 μM. DMSO only was added to control incubation mixtures. The mixture was incubated for 5 min at 23 °C, which resulted in loss of activity of greater than 90%. The inactivation was terminated by transferring the reaction mixture to a Bio Spin 6 Tris column that had been equilibrated with the incubation buffer. After the mixture was centrifuged at 1000*g* for 4 min at 4 °C, 10 μL of the solution was used to assay for protein concentration (*22*) and NAT1 activity. To the remaining solution, 20 μL of 10% acetic acid was added slowly, followed by 1 μL of 1% TFA. The mixture was centrifuged at 16 000*g* for 5 min at 4 °C and was subjected to rpHPLC on a Vydac C4 MS column (214MS54, 4.6 mm × 250 mm). A stepwise isocratic elution with a flow rate of 1 mL/min was used. Solvent A was 5% acetonitrile in 0.01% TFA. Solvent B was 95% acetonitrile in 0.01% TFA. The column was eluted with 100% A (2 min), 35% B (4 min), 65% B (7 min), and 100% B (5 min). The eluate was monitored at 220 and 280 nm. NAT1 eluted at 10.4 min. The protein-containing fractions were stored at −80 °C.

Inactivation of NAT1 by N-OH-AAF in the Presence of Low Molecular Weight Nucleophiles. To NAT1 (80 μg, 48 μM) in potassium phosphate buffer (48 μL, 20 mM, 1 mM EDTA, 10% glycerol, 0.1 mM DTT, pH 7.4) was added either L-cysteine or glutathione dissolved in 1 μL of water. The final concentration of either nucleophile was 10 mM. The mixture was incubated for 2 min at 23 °C followed by addition of 1 μL of N-OH-AAF in DMSO. The final concentration of N-OH-AAF was 0.5 mM. The mixture was incubated for an additional 5 min at 23 °C, at which time 50 μL of the incubation buffer was added to make the final volume 100 μL. The reaction was terminated by transferring the mixture to a modified Bio Spin 6 Tris column that contained twice the usual quantity of gel matrix and had been equilibrated with the incubation buffer. After the mixture was centrifuged at 1000*g* for 4 min at 4 °C, the concentration of NAT1 in the eluate was determined by the Bradford assay (*22*), and the residual transacetylation activity was assayed. The remaining solution was subjected to rpHPLC chromatography as described above for N-OH-AAF-treated NAT1. The protein-containing fractions were stored at −80 °C.

Pepsin Digestion of N-OH-AAF-Treated NAT1. To NAT1 (220 μg, 67 μM) in potassium phosphate buffer (98 μL, 20 mM, 1 mM EDTA, 10% glycerol, 0.1 mM DTT, pH 7.4) was added N-OH-AAF dissolved in 2 μL of DMSO. The final concentration of N-OH-AAF was 0.5 mM. The mixture was incubated for 5 min at 23 °C, which resulted in loss of activity of greater than 90%. The reaction was terminated by transferring the mixture to a Bio Spin 6 Tris column, which had been equilibrated with the incubation buffer. After the mixture was centrifuged at 1000*g* for 4 min at 4 °C, 10 μL of the solution was used to assay for protein concentration and NAT1 activity. To 98 μL of the remaining solution, 2 μL of 6 N HCl was added to lower the pH to 1−1.5. The digestion was initiated by adding pepsin dissolved in 0.1 N HCl (0.8 μL); the final concentration of pepsin was 2 μg/100 μL. After the digestion mixture was incubated at 37 °C for 3.5 h, 10 μL of acetonitrile and 1 μL of 1% TFA solution were added. Half of the mixture was removed and stored at −80 °C for differential MALDI TOF MS peptide mapping. The remaining mixture was centrifuged at 16 000*g* for 5 min at 4 °C, and the peptides were fractionated by rpHPLC on a Vydac C18 MS column (218MS21, 2.1 mm × 250 mm) at a flow rate of 0.2 mL/min. Solvent A was 5% acetonitrile in 0.01% TFA. Solvent B was 95% acetonitrile in 0.01% TFA. A stepwise gradient elution was used as follows: 0% B (0−5 min), 0−40% B (5−65 min), 40−70% B (65−95 min), and 70−100% B (95−110 min). The fractions were monitored at 220 and 280 nm and were collected at 1.0 min intervals. The peptide-containing fractions were screened by MALDI TOF MS, and those that contained adducted peptides were analyzed by MALDI Q-TOF MS, and the adducted peptides were sequenced by tandem MS. A NAT1 control digest was obtained similarly, to which DMSO had been added instead of the N-OH-AAF DMSO solution.

Pepsin Digestion of 2-Nitrosofluorene-Treated NAT1. The procedures were identical to those described for N-OH-AAF-treated NAT1 except that the final concentration of 2-nitrosofluorene was 250 μM.

Endopeptidase Glu-C Digestion of N-OH-AAF-Treated NAT1. To NAT1 (80 μg, 48 μM) in potassium phosphate buffer (49 μL, 20 mM, 1 mM EDTA, 10% glycerol, 0.1 mM DTT, pH 7.4) was added N-OH-AAF dissolved in 1 μL of DMSO. The final concentration of N-OH-AAF was 0.5 mM. The mixture was incubated for 5 min at 23 °C, which resulted in loss of activity of greater than 90%. After the incubation, 50 μL of the incubation buffer was added. The reaction was terminated by transferring the reaction mixture to a Bio Spin 6 Tris column, which had been equilibrated with the incubation buffer. After the mixture was centrifuged at 1000*g* for 4 min at 4 °C, 10 μL of the solution was used to assay for protein concentration and NAT1 activity. The digestion was initiated by adding 5 μL of endopeptidase Glu-C in water to 95 μL of solution containing N-OH-AAF-treated NAT1. The final concentration of the protease was 5 μg/100 μL. After 20 h of incubation at 37 °C, 10 μL of acetonitrile and 1 μL of 1% TFA were added to the mixture. Part of the mixture (50 μL) was removed and stored at −80 °C for differential MALDI TOF MS mapping. The remaining mixture was centrifuged at 16 000*g* for 5 min at 4 °C, and the peptides were fractionated by rpHPLC on a Vydac C18 MS column (218MS21, 2.1 mm × 250 mm) at a flow rate of 0.2 mL/min. Solvent A was 5% acetonitrile in 0.01% TFA. Solvent B was 95% acetonitrile in 0.01% TFA. A stepwise gradient elution was used as follows: 0% B (0−5 min), 0−40% B (5−65 min), 40−70% B (65−95 min), and 70−100% B (95−110 min). The fractions were monitored at 220 and 280 nm and were collected at 1.5 min intervals. The peptide-containing fractions were screened by MALDI TOF MS, and the fractions that contained adducted peptides were analyzed by MALDI Q-TOF MS, and the adducted peptides were sequenced by tandem MS. A NAT1 control digest was obtained similarly, to which DMSO had been added instead of the N-OH-AAF DMSO solution.

Endopeptidase Lys-C Digestion of Adducted Peptide DQIVRKKRGGWCLQVNHLLY. The volume of the rpHPLC fraction containing the peptide (∼200 μL) was reduced to about 50 μL by centrifugation under vacuum with heating (37 °C). The pH of the solution was adjusted to ∼8.5 by adding an appropriate amount of 1 M ammonium bicarbonate dissolved in water. The digestion was initiated by adding 2 μg of endopeptidase Lys-C in water (2 μL). After a 4 h incubation at 37 °C, the digestion was terminated by acidification with 1% TFA to pH ∼ 2−3, followed by addition of 5 μL of acetonitrile. The peptides were analyzed by MALDI TOF MS, and the adducted peptide was sequenced by MALDI Q-TOF MS/MS.

ESI Q-TOF MS of Unmodified and Modified NAT1. Protein masses were obtained by direct infusion with a QSTAR Q-TOF mass spectrometer from Applied Biosystems, Inc. The IonSpray source was used with an ESI infusion flow rate of 25 μL/min (acetonitrile:water, 65:35, 0.01% TFA). The ESI voltage was 5000 V; mass spectra were the average of 300 scans collected in the positive ion mode. The TOF region acceleration voltage was 4 kV. The injection pulse repetition rate was 6.0 kHz. The series of multiply charged protein peaks from 700 to 3000 *m*/*z* were deconvoluted to provide protein zero-charge mass with the Bayesian Reconstruct tool in the ABI BioAnalyst software package, which is based on maximum entropy theory.

MALDI TOF MS Screening of Peptides. MALDI TOF MS data were obtained with a Bruker Biflex III instrument, equipped with a N_2 laser (337 nm, 3 nanosecond pulse length) and a microchannel plate detector. Data were collected in the reflectron mode, positive polarity, with an accelerating potential of 19 kV. Samples were prepared with a methanol stock solution of α-cyano-4-hydroxycinnamic acid (Hewlett-Packard) diluted 1:1 with 50:50 acetonitrile:Nanopure water containing 0.1% TFA. External calibration was performed with human angiotensin II (monoisotopic [MH^+] *m*/*z* 1046.5; Sigma) and adrenocorticotropin hormone (ACTH) fragment 18-39 (monoisotopic [MH^+] *m*/*z* 2465.2; Sigma).

MALDI Q-TOF MS/MS of Adducted Peptides. Prior to analysis, a portion of the peptide mixtures was desalted with Millipore C18 ZipTips according to the protocol described by Millipore for peptides in solution with a high concentration of salt. Peptides in HPLC fractions were directly applied onto the target without an additional desalting step. Full scans of the peptide mixture from 600 to 3500 *m*/*z* and tandem mass spectral data for selected ions were collected on a QSTAR Pulsar *i* (Applied Biosystems Inc., Foster City, California) Q-TOF mass spectrometer with an orthogonal MALDI source and DHB as matrix (2,5-dihydroxybenzoic, Agilent Technologies, Palo Alto, CA). The TOF region acceleration voltage was 4 kV, and the injection pulse repetition rate was 6.0 kHz. Laser pulses were generated with a nitrogen laser at 337 nm, 33 μJoules of laser energy with a laser repetition rate of 20 Hz. Mass spectra were the average of approximately 100 laser shots collected in positive mode. External calibration was performed with human angiotensin II (monoisotopic [MH^+] *m*/*z* 1046.5; Sigma) and ACTH fragment 18-39 (monoisotopic [MH^+] *m*/*z* 2465.2; Sigma).

MS Data Analysis. Theoretical masses of protein, peptides, and fragment ions were generated with Protein Prospector (http://prospector.ucsf.edu/).

Results

ESI Q-TOF MS Analysis of N-OH-AAF-Treated NAT1. We demonstrated previously that a number of N-arylhydroxamic acids, including N-OH-AAF, are irreversible inactivators of NATs (*10*, *15*, *19*). It is widely accepted that most N-acetoxy esters, produced from N-arylhydroxamic acids by the NAT-catalyzed N,OAT reaction (Figure 1c), are precursors to N-arylnitrenium ions, which are ultimately responsible for arylamine−nucleophile adduct formation (*7*, *25*). Thus, conversion of N-OH-AAF to an N-acetoxy ester would be expected to lead to covalent binding of 2-AF to NAT1 and would result in a mass increment of 179 Da.

The ESI Q-TOF MS of native (untreated) NAT1 (Figure 2a) reveals a molecular mass of 33 899.9 Da, which matches the theoretical mass of 33 900 Da, including the four additional amino acids (Gly, Thr, Gln, and Leu) present at the N terminus of the recombinant protein. After incubation with N-OH-AAF, however, NAT1 yields a mass spectrum (Figure 2b) that contains a very small peak (33 899.4 Da), which corresponds to the native protein, and a major peak (34 094.7 Da), indicating a mass increment of 195.3 Da rather than 179 Da. Assuming that one proton from NAT1 and one proton from the reactant are lost during adduct formation, the mass increase of 195 corresponds to adduction of 2-AF and an atom of oxygen. Two minor, but significant, peaks appear at 34 273.4 and 34 290.2 Da, corresponding to mass increases of 178.7 and 195.5 Da, respectively, relative to the 34 094.7 Da peak. The mass shift of 178.7 Da indicates adduction of 2-AF (theoretical increase, 179 Da; Figure 3c), and the increase of 195.5 Da apparently indicates another addition of 2-AF and an atom of oxygen.

Insight into the identity of the molecular species responsible for the mass increment of 195.3 Da was obtained when NAT1, which had been incubated with N-OH-AAF, was subjected to rpHPLC in which 2% formic acid, rather than 0.01% TFA, was used as the ion-pairing reagent. The most intense peak in the mass spectrum (Figure 2c) of adducted protein that had been eluted with formic acid was 33 930.9 Da, a mass increase of 31.9 Da over that of NAT1. Also, as shown in Figure 2c, the peak of mass increment 195 Da (34 093.5 Da), relative to the mass of the native protein, was substantially less intense than the corresponding peak in Figure 2b, suggesting that the mass increase of 31.9 Da may represent a sulfinic acid residue (Figure 3b), which could have been

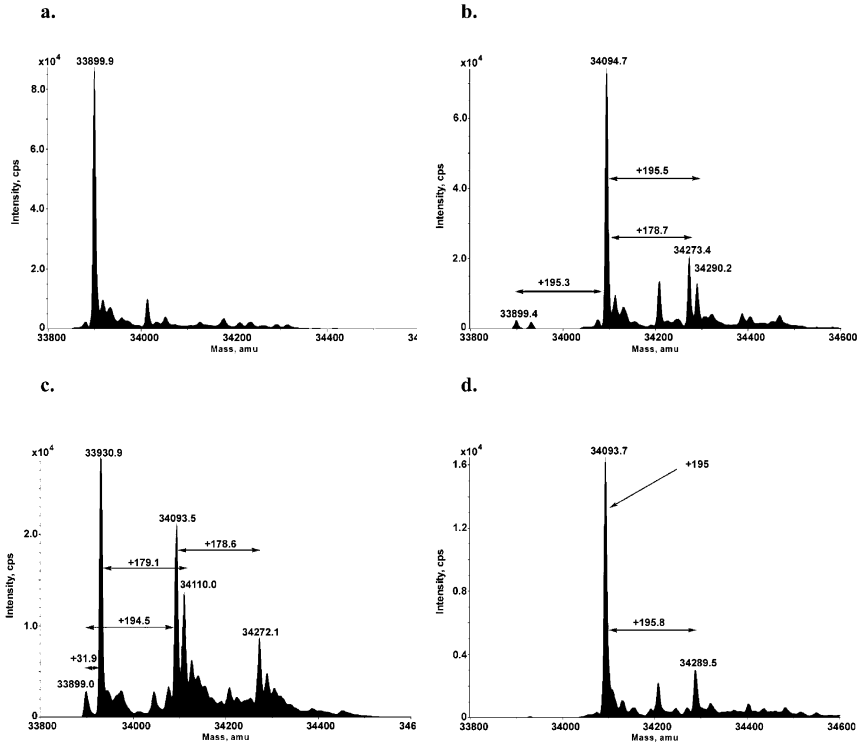

Figure 2. Deconvoluted ESI Q-TOF mass spectra: (a) native NAT1; (b) N-OH-AAF-inactivated NAT1; (c) N-OH-AAF-inactivated NAT1 after rpHPLC with formic acid as the ion-pairing reagent; and (d) 2-nitrosofluorene-inactivated NAT1.

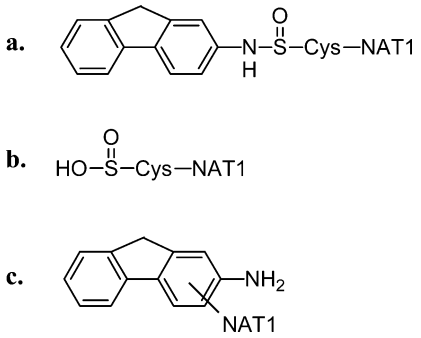

Figure 3. (a) (2-Fluorenyl)-sulfinamide-NAT1 adduct; (b) sulfinic acid-NAT1 modification; and (c) 2-AF-NAT1 adduct.

produced by hydrolysis of a sulfinamide adduct (Figure 3a). Although it is possible that a sulfinic acid residue could result from oxidation of a cysteine thiol group, no peaks showing a 32 Da mass shift were present in the mass spectra of NAT1 control samples that had been subjected to the same incubation and chromatographic conditions as NAT1 that had been incubated with N-OH-AAF. The 34 110.0 Da peak in Figure 2c corresponds to a mass increase of 179.1 Da (2-AF, Figure 3c) relative to the 33 930.9 Da peak, and the peak at 34 272.1 Da corresponds to the addition of 178.6 Da (2-AF, Figure 3c) relative to the 34 093.5 Da peak.

ESI Q-TOF MS of 2-Nitrosofluorene-Treated NAT1. The data presented in Figure 2a−c suggest that the major adduct formed upon incubation of NAT1 with N-OH-AAF is a (2-fluorenyl)sulfinamide. Because it is well-established that arylnitroso compounds react with biological thiols to yield sulfinamide conjugates (*26*−*28*), 2-nitrosofluorene was synthesized and incubated with NAT1 to determine its effectiveness as an inhibitor of the enzyme. As little as 4-fold excess of 2-nitrosofluorene caused 90−100% loss of NAT1 activity within 30 s (data not shown), and the activity was not regained after removal of excess inhibitor by gel filtration. The ESI Q-TOF mass spectrum of 2-nitrosofluorene-treated NAT1 (Figure 2d) exhibits a single major peak of 34 093.7 Da, corresponding to a mass increment of 195 Da relative to the native protein, and a minor peak (34 289.5 Da), indicating an addition of 195.8 Da to the 34 093.7 Da protein. Both peaks can be interpreted as resulting from the reaction of 2-nitrosofluorene with cysteine thiols to yield sulfinamide adducts. No peaks corresponding to a mass increase of 179 Da were observed, indicating that no 2-AF adducts were formed when 2-nitrosofluorene reacted with NAT1.

Proteolysis of N-OH-AAF-Treated NAT1 and MALDI Q-TOF MS/MS Analysis. Digestion with either trypsin or a combination of trypsin and endoproteinase Glu-C provided incomplete sequence coverage of NAT1, as judged by MALDI TOF MS analysis, and did not yield adducted peptides, according to the results of differential peptide mapping of whole digests. It was noted, however, that the rpHPLC traces of all digests of N-OH-AAF-modified NAT1 exhibited a unique intense peak, which proved to have a retention time and UV spectrum identical with that of 2-AF (data not shown). The latter result provided further support for the presence of a hydrolytically labile adduct, such as a sulfinamide.

Digestion of NAT1 with pepsin provided more complete coverage of the sequence, and although pepsin-catalyzed proteolysis exhibits somewhat variable specificity as compared to other commonly used endopeptidases, the results were consistent and reproducible under well-controlled conditions. MALDI TOF MS of the pepsin digests of control NAT1 and N-OH-AAF-modified NAT1 revealed modified peptides with monoisotopic masses of 2458.32 (Figure 4b) and 1740.92 Da (Figure 5b), which were not present in pepsin digests of native NAT1 (Figures 4a and 5a). Furthermore, as seen in Figure 4a, a peptide of monoisotopic mass 2426.11 Da, correspond-

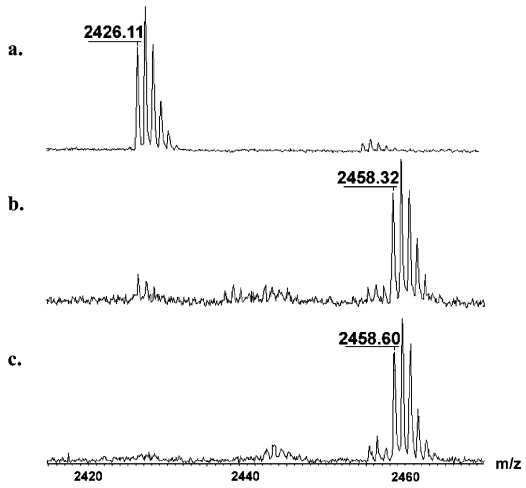

Figure 4. Segments of the MALDI TOF mass spectra of pepsin digests of (a) native NAT1; (b) N-OH-AAF-inactivated NAT1; and (c) 2-nitrosofluorene-inactivated NAT1.

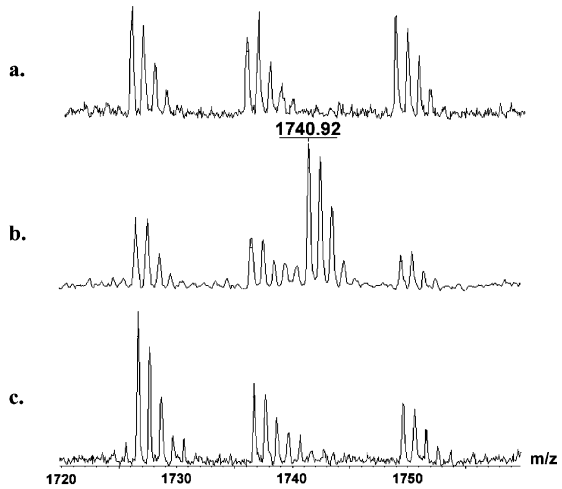

Figure 5. Segments of the MALDI TOF mass spectra of pepsin digests of (a) native NAT1; (b) N-OH-AAF-inactivated NAT1; and (c) 2-nitrosofluorene-inactivated NAT1.

ing to the peptide sequence DQIVRKKRGGWCLQVNHL-LY (Asp57-Tyr76; theoretical mass, 2426.32 Da) was present in the control digest but not in the pepsin digest of NAT1 that had been incubated with N-OH-AAF (Figure 4b).

The rpHPLC fraction that contained the peptide of mass 2458.32 Da (Figure 4b) was concentrated and subjected to MALDI Q-TOF MS and MALDI Q-TOF MS/MS analysis, the results of which indicated a modified (+32 Da) sequence of DQIVRKKRGGWCLQVNHLLY, but the data were of insufficient quality to identify the modified residue unequivocally. Therefore, the rpHPLC fraction containing the peptide of mass 2458.32 Da was treated with endopeptidase Lys-C to yield two new peptides consisting of the modified sequence RGGW-CLQVNHLLY (Arg64-Tyr 76, 1590.92 Da) and the unmodified sequence DQIVRKK (Asp57-Lys63, 886.61 Da). MALDI Q-TOF MS/MS of the peptide of mass 1590.92 indicated that Cys68 was the modified residue, with the b4 ion (457.23 *m*/*z*) and the b5 ion (592.23 *m*/*z*) being distinctly diagnostic (Figure 6 and Table 1). The b1−b4 ions were in agreement with the theoretical masses, and

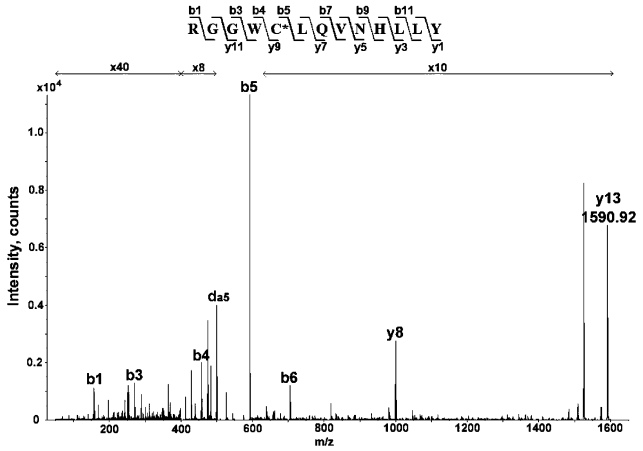

Figure 6. MALDI Q-TOF tandem mass spectrum of the 1590.92 Da peptide obtained by sequential pepsin and endopeptidase Lys-C digestion of N-OH-AAF-inactivated NAT1.

the b5 ion was 32 Da greater than its theoretical mass. Additional evidence for the presence of a sulfinic acid functional group was provided by the apparent da5 ion at 500.27 *m*/*z*, which may have resulted from side chain cleavage, causing a neutral loss of SO_2 from an a5 ion (*29*). The a5 ion, however, was of such low intensity that it could not be assigned unequivocally.

MALDI Q-TOF MS of the rpHPLC fraction containing the peptide of mass 1740.92 Da (Figure 5b) identified the modified (+179 Da) sequence LEKNTYRKIYSF (Leu181-Phe192; unmodified theoretical mass, 1561.84 Da). Subjecting the peptide to MS/MS yielded the results shown in Table 2 and Figure 7. The b5 ion (586.31 *m*/*z*) and the b6 ion (928.47 *m*/*z*) allowed unequivocal designation of Tyr186 as being covalently bonded with 2-AF (Figure 3c, +179 Da).

NAT1 that had been inactivated with N-OH-AAF was also subjected to treatment with endopeptidase Glu-C in an effort to identify any additional adducted amino acid residues. MALDI Q-TOF MS comparison of the resulting digest with a control digest identified a new peak of 1604.66 Da (Figure 8a,b), which corresponded to the modified (+179 Da) sequence RIGYNNPVYTLD (Arg9-Asp20; unmodified theoretical mass, 1424.72 Da). The tandem MS data for the adducted peptide are shown in Table 3 and Figure 9. The b8 ion (914.57 *m*/*z*) and the b9 ion (1256.66) are diagnostic and verify that Tyr17 is covalently bound to 2-AF.

Proteolysis of 2-Nitrosofluorene-Treated NAT1 and MALDI Q-TOF MS/MS Analysis. NAT1 that had been incubated with 2-nitrosofluorene was subjected to pepsin-catalyzed proteolysis, and the resulting digest was analyzed by MALDI TOF MS. A modified (+32 Da) peptide of mass 2458.60 Da (Figure 4c), corresponding to the sequence DQIVRKKRGGWCLQVNHLLY (Asp57-Tyr76; unmodified theoretical mass, 2426.32 Da), was identified. The rpHPLC fraction containing the modified peptide was treated with endopeptidase Lys-C, which produced the modified (+32 Da) peptide of mass 1590.90 Da, corresponding to the sequence RGGWCLQVNHLLY (Arg64-Tyr76). MALDI Q-TOF MS/MS of the latter peptide allowed the assignment of Cys68 as the modified residue, with the b4 ion (457.23 *m*/*z*) and the b5 ion (592.22 *m*/*z*) being diagnostic for the added mass of 32 Da (Table 4 and Figure 10). There were no peptides present in the proteolytic digests of 2-nitrosofluorene-

Table 1. Theoretical and Experimental *m/z* for b and y Ions Obtained by MALDI Q-TOF MS/MS of RGGWC*LQVNHLLY Derived from N-OH-AAF-Treated NAT1[a]

b ions	experimental *m/z*	theoretical *m/z*	sequence	theoretical *m/z*	experimental *m/z*	y ions
b1	157.11	157.11	R GGWC*LQVNHLLY	1434.68		y12
b2		214.13	RG GWC*LQVNHLLY	1377.66		y11
b3	271.15	271.15	RGG WC*LQVNHLLY	1320.64		y10
b4	457.23	457.23	RGGW C*LQVNHLLY	1134.56		y9
b5	592.23	592.23	RGGWC* LQVNHLLY	999.56	999.58	y8
b6	705.41	705.31	RGGWC*L QVNHLLY	886.48	886.48	y7
b7	833.39	833.37	RGGWC*LQ VNHLLY	758.42	758.44	y6
b8	932.48	932.44	RGGWC*LQV NHLLY	659.35	659.36	y5
b9	1046.52	1046.48	RGGWC*LQVN HLLY	545.31		y4
b10		1183.54	RGGWC*LQVNH LLY	408.25		y3
b11		1296.63	RGGWC*LQVNHL LY	295.17		y2
b12		1409.71	RGGWC*LQVNHLL Y	182.08		y1

[a] The modified cysteine residue (Cys68) is designated C*. The complete mass spectrum is shown in Figure 6.

Table 2. Theoretical and Experimental *m/z* for b and y Ions Obtained by MALDI Q-TOF MS/MS of LEKNTY*RKIYSF Derived from N-OH-AAF-Treated NAT1[a]

b ions	experimental *m/z*	theoretical *m/z*	sequence	theoretical *m/z*	experimental *m/z*	y ions
b1		114.09	L EKNTY*RKIYSF	1627.83		y11
b2	243.13	243.13	LE KNTY*RKIYSF	1498.78	1498.89	y10
b3	371.25	371.23	LEK NTY*RKIYSF	1370.69	1370.77	y9
b4	485.27	485.27	LEKN TY*RKIYSF	1256.65	1256.71	y8
b5	586.31	586.32	LEKNT Y*RKIYSF	1155.6	1155.61	y7
b6	928.47	928.46	LEKNTY* RKIYSF	813.46		y6
b7	1084.56	1084.56	LEKNTY*R KIYSF	657.36	657.38	y5
b8	1212.68	1212.65	LEKNTY*RK IYSF	529.26		y4
b9	1325.81	1325.74	LEKNTY*RKI YSF	416.18		y3
b10	1488.89	1488.8	LEKNTY*RKIY SF	253.12	253.13	y2
b11	1575.9	1575.83	LEKNTY*RKIYS F	166.09		y1

[a] The modified tyrosine residue (Tyr186) is designated Y*. The complete mass spectrum is shown in Figure 7.

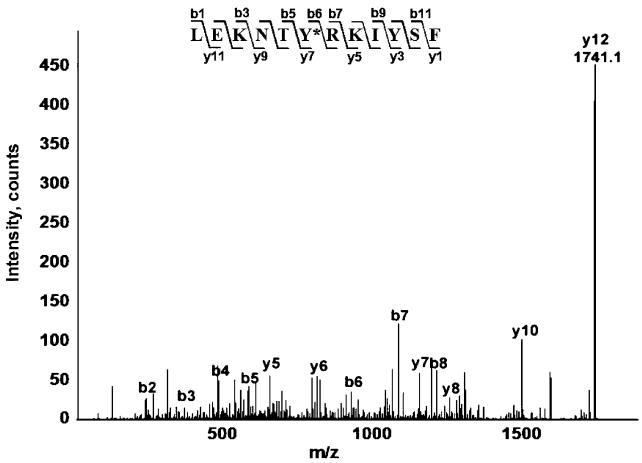

Figure 7. MALDI Q-TOF tandem mass spectrum of the 1740.92 Da peptide obtained by pepsin digestion of N-OH-AAF-inactivated NAT1.

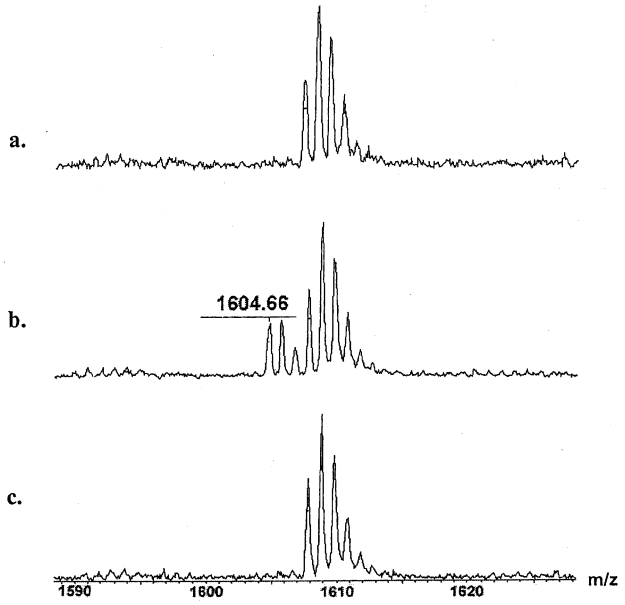

Figure 8. Segments of the MALDI TOF mass spectra of the endopeptidase Glu-C digests of (a) native NAT1; (b) N-OH-AAF-inactivated NAT1; and (c) 2-nitrosofluorene-inactivated NAT1.

inactivated NAT1 that were the result of covalent adduction of either Tyr186 or Tyr17 with 2-AF (Figures 5c and 8c), nor were 2-AF adducts of any other peptides detected.

The mass spectra of NAT1 that had been inactivated by either N-OH-AAF or 2-nitrosofluorene contained minor peaks indicating the presence of a second adduct of +195 Da (Figure 2b,d). The adduct could not be identified, even after careful analysis of proteolytic digests obtained from incubations with pepsin, trypsin/endopeptidase Glu-C, endopeptidase Glu-C, and endopeptidase Asp-N. Although the most likely site of such an adduct is a cysteine residue, none of the five cysteines of NAT1 was found to be modified, other than Cys68. It is possible that the unidentified adduct of 195 Da (Figure 2b,d) is a semimercaptal, an intermediate in sulfinamide formation (*26*). A semimercaptal would not be expected to be stable under proteolysis and HPLC conditions.

Effect of N-OH-AAF on NAT1 in the Presence of Cysteine and GSH. The results described above provide definitive evidence that inactivation of NAT1 in the presence of N-OH-AAF results from reaction of 2-nitrosofluorene with the catalytically essential Cys68. Because nucleophilic thiols, such as cysteine and GSH, react readily with arylnitroso compounds, their effect on

Table 3. Theoretical and Experimental *m/z* for b and y Ions Obtained by MALDI Q-TOF MS/MS of RIGYNNPVY*TLD Derived from N-OH-AAF-Treated NAT1[a]

b ions	experimental *m/z*	theoretical *m/z*	sequence	theoretical *m/z*	experimental *m/z*	y ions
b1	157.25	157.11	R IGYNNPVY*TLD	1447.69		y11
b2	270.35	270.19	RI GYNNPVY*TLD	1334.61		y10
b3	327.37	327.21	RIG YNNPVY*TLD	1277.58		y9
b4	490.42	490.28	RIGY NNPVY*TLD	1114.52		y8
b5	604.46	604.32	RIGYN NPVY*TLD	1000.48		y7
b6	718.49	718.36	RIGYNN PVY*TLD	886.43		y6
b7	815.54	815.42	RIGYNNP VY*TLD	789.38		y5
b8	914.57	914.48	RIGYNNPV Y*TLD	690.31		y4
b9	1256.66	1256.62	RIGYNNPVY* TLD	348.18		y3
b10	1357.67	1357.67	RIGYNNPVY*T LD	247.13		y2
b11	1470.81	1470.75	RIGYNNPVY*TL D	134.04		y1

[a] The modified tyrosine residue (Tyr17) is designated Y*. The complete mass spectrum is shown in Figure 9.

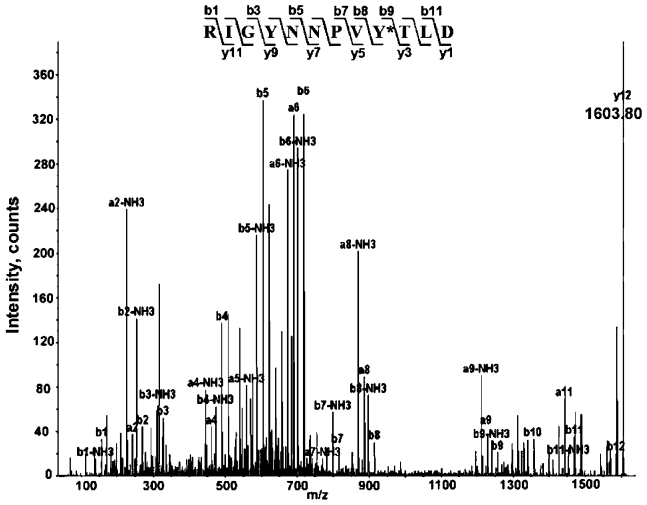

Figure 9. MALDI Q-TOF tandem mass spectrum of the 1604.66 Da peptide obtained by endopeptidase Glu-C digestion of N-OH-AAF-inactivated NAT1.

both N-OH-AAF-induced inactivation of NAT1 and adduct formation was examined. As seen in Figure 11, incubation with N-OH-AAF (0.5 mM) caused a 90% loss of NAT1 activity, but in the presence of cysteine (10 mM), only a 30% reduction in enzyme activity occurred. In contrast to the effect of cysteine, GSH (10 mM) provided no protection of NAT1 from inactivation by N-OH-AAF (Figure 11). The effects of cysteine and GSH on NAT1 activity are reflected by the ESI Q-TOF MS data obtained with NAT1 that had been treated with N-OH-AAF (Figure 12). As seen in Figure 12a, after incubation of NAT1 with N-OH-AAF in the presence of cysteine, the most intense peak is that of native NAT1 (33 896.7 Da), whereas the peaks corresponding to the (2-fluorenyl)-sulfinamide adduct (34 091.7 Da) and the 2-AF adduct (34 271.1 Da) represent minor components of the spectrum. The mass spectrum of NAT1 that had been incubated with N-OH-AAF in the presence of GSH (Figure 12b), however, was virtually identical to the spectrum obtained from the same experiment conducted in the absence of GSH (Figure 2b). That is, the most intense peak in Figure 12b is the sulfinamide adducted NAT1 (34 091.8 Da), and the peak representing native NAT1 (38 396.7 Da) is of very low intensity. The only noticeable effect of GSH on adduct formation is the absence from Figure 12b of a second minor peak (34 290.2 Da), corresponding to a second addition of 195 Da, seen in Figure 2b.

Discussion

Two NAT isozymes, NAT1 and NAT2, are found in both human and hamster tissues. The deduced amino acid sequence identity among human and hamster NATs is 69−82%, and although the substrate selectivity of human NAT1 corresponds in general to that of hamster NAT2, the capacity for catalysis of the AcCoA-independent conversion of N-arylhydroxamic acids to reactive N-acetoxy esters (N,OAT activity, Figure 1c) is exhibited primarily by the NAT1 isozymes (*19*, *30*, *31*). In this study, we have used purified hamster recombinant NAT1 and Q-TOF MS to gain insight into the molecular mechanism of the irreversible inactivation that results from NAT1-catalyzed bioactivation of N-OH-AAF.

ESI Q-TOF mass spectrometric analysis of NAT1 that had been incubated with N-OH-AAF revealed that the major adduct (+195 Da) was a hydrolytically labile sulfinamide (Figure 3a). The sulfinamide adduct remained intact when 0.01% TFA was used as an ion-pairing reagent during chromatographic preparation of the adducted protein for MS analysis. The sulfinamide, however, underwent extensive hydrolysis to yield 2-AF and a protein with a mass of 31.9 Da greater than that of NAT1 when formic acid was used rather than TFA. The sulfinamide adduct underwent complete hydrolysis when the adducted protein was subjected to proteolysis and rpHPLC, regardless of which protease was used, the pH of the digestion mixture, or the chromatographic conditions. Hydrolysis of a sulfinamide is expected to yield, in addition to the amine (2-AF), a sulfinic acid (*32*, *33*). The hydrolytic formation of a modified protein with a mass of 31.9 Da greater than that of NAT1 is consistent with the presence of a sulfinic acid residue (Figure 3b).

Verification of the structural identity of the major NAT1 adduct formed during incubation with N-OH-AAF was obtained by treatment of NAT1 with 2-nitrosofluorene, which is known to generate (2-fluorenyl)sulfinamides upon reaction with thiols (*27*). The reaction between NAT1 and 2-nitrosofluorene resulted not only in rapid inactivation of the enzyme but also in formation of a major adduct with a mass of 195 Da greater than that of NAT1, identical to the result obtained with N-OH-AAF.

MALDI Q-TOF MS/MS of the principal modified peptide present in the pepsin digest obtained from NAT1 that had undergone inactivation with N-OH-AAF revealed that the modified amino acid residue was the catalytically essential Cys68. All NATs, including the prokaryotic enzymes, utilize a nucleophilic cysteine thiol as an acceptor for the acetyl group provided by AcCoA,

Table 4. Theoretical and Experimental *m/z* for b and y Ions Obtained by MALDI Q-TOF MS/MS of RGGWC*LQVNHLLY Derived from 2-Nitrosofluorene-Treated NAT1[a]

b ions	experimental *m/z*	theoretical *m/z*	sequence	theoretical *m/z*	experimental *m/z*	y ions
b1	157.1	157.11	R GGWC*LQVNHLLY	1434.68		y12
b2		214.13	RG GWC*LQVNHLLY	1377.66		y11
b3	271.14	271.15	RGG WC*LQVNHLLY	1320.64		y10
b4	457.23	457.23	RGGW C*LQVNHLLY	1134.56		y9
b5	592.22	592.23	RGGWC* LQVNHLLY	999.56	999.58	y8
b6	705.39	705.31	RGGWC*L QVNHLLY	886.48		y7
b7	833.44	833.37	RGGWC*LQ VNHLLY	758.42		y6
b8	932.47	932.44	RGGWC*LQV NHLLY	659.35	659.36	y5
b9	1046.46	1046.48	RGGWC*LQVN HLLY	545.31		y4
b10		1183.54	RGGWC*LQVNH LLY	408.25		y3
b11		1296.63	RGGWC*LQVNHL LY	295.17		y2
b12		1409.71	RGGWC*LQVNHLL Y	182.08		y1

[a] The modified cysteine residue (Cys68) is designated C*. The complete mass spectrum is shown in Figure 10.

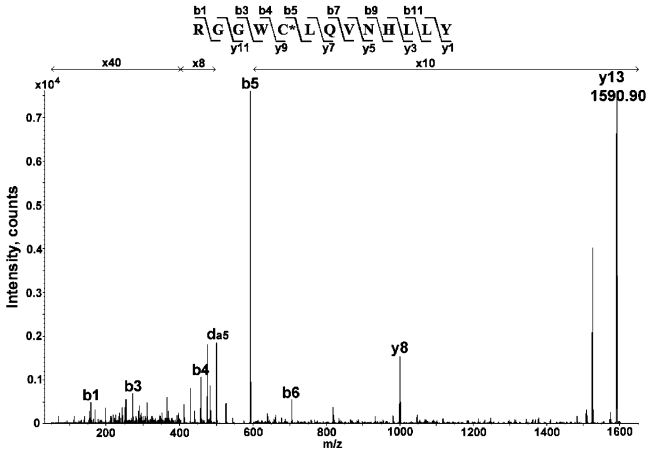

Figure 10. MALDI Q-TOF tandem mass spectrum of the 1590.90 Da peptide obtained by sequential pepsin and endopeptidase Lys-C digestion of 2-nitrosofluorene-inactivated NAT1.

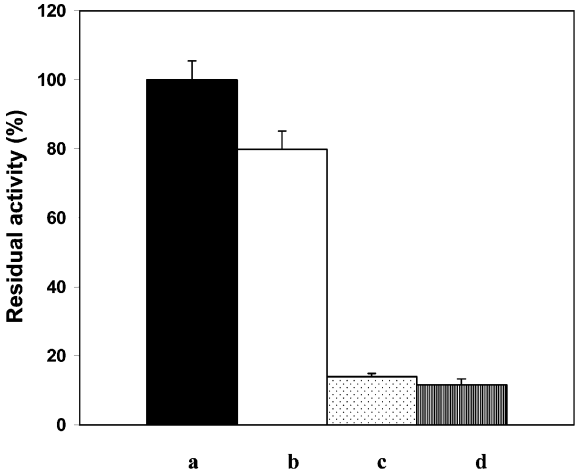

Figure 11. Effect of cysteine (10 mM) and GSH (10 mM) on the inactivation of NAT1 (0.048 mM) by N-OH-AAF (0.5 mM). Incubations were conducted as described under the Experimental Procedures. Control activity was 19.9 ± 0.4 μmol/mg protein/min (mean ± SD, $n = 3$). All results are expressed as the mean ± SD for three experiments. (a) Control; (b) N-OH-AAF + cysteine; (c) N-OH-AAF + GSH; and (d) N-OH-AAF. Results a−c are significantly different from one another ($P < 0.01$), whereas c and d are not significantly different ($P > 0.05$).

prior to transfer of the acetyl group to an arylamine or an arylhydroxylamine (Figure 1a,b) (*34*, *35*).

The finding that 2-nitrosofluorene is the reactant responsible for inactivation of NAT1 was unexpected. The process of NAT1-catalyzed bioactivation of N-arylhydroxamic acids, such as N-OH-AAF, is believed to involve the transfer of the acetyl group to Cys68 of NAT1, generating an acetyl−enzyme intermediate (AcNAT1, Scheme 1) (*7*). The resulting N-arylhydroxylamine (N-OH-AF) then undergoes O-acetylation to produce an N-acetoxyarylamine (N-OAc-AF), which upon heterolytic N−O bond cleavage, generates resonance-stabilized N-arylnitrenium ions (Scheme 1). The latter reactants are believed to be the electrophiles that are primarily responsible for arylamine−DNA adduct formation (*25*, *36*). The sulfinamide adduct formed with the thiol group of Cys68 does not arise from reaction with a 2-aminofluorenylnitrenium ion, which would result in adduction of 2-AF, but from reaction with 2-nitrosofluorene. The most likely source of 2-nitrosofluorene is through oxidation of N-OH-AF, which is formed when NAT1 deacylates N-OH-AAF

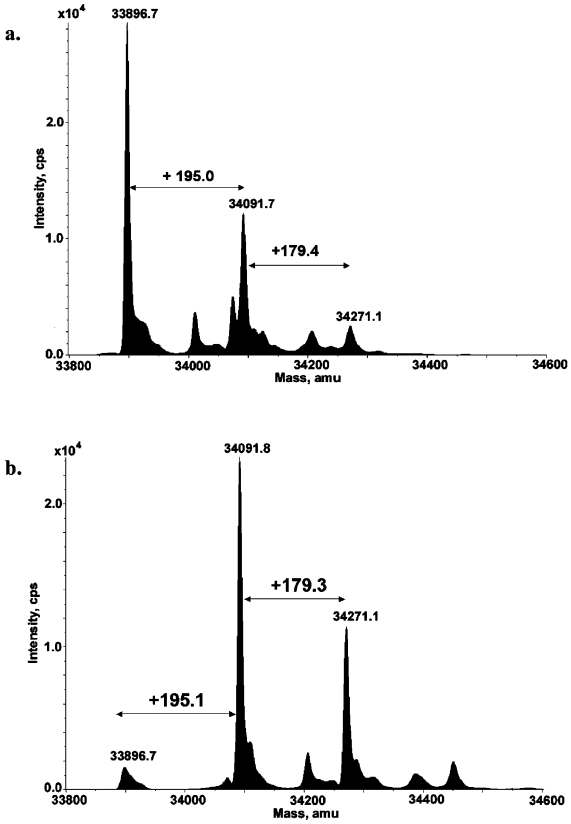

Figure 12. Deconvoluted ESI Q-TOF mass spectra of NAT1 treated with N-OH-AAF in the presence of (a) cysteine and (b) GSH.

Scheme 1

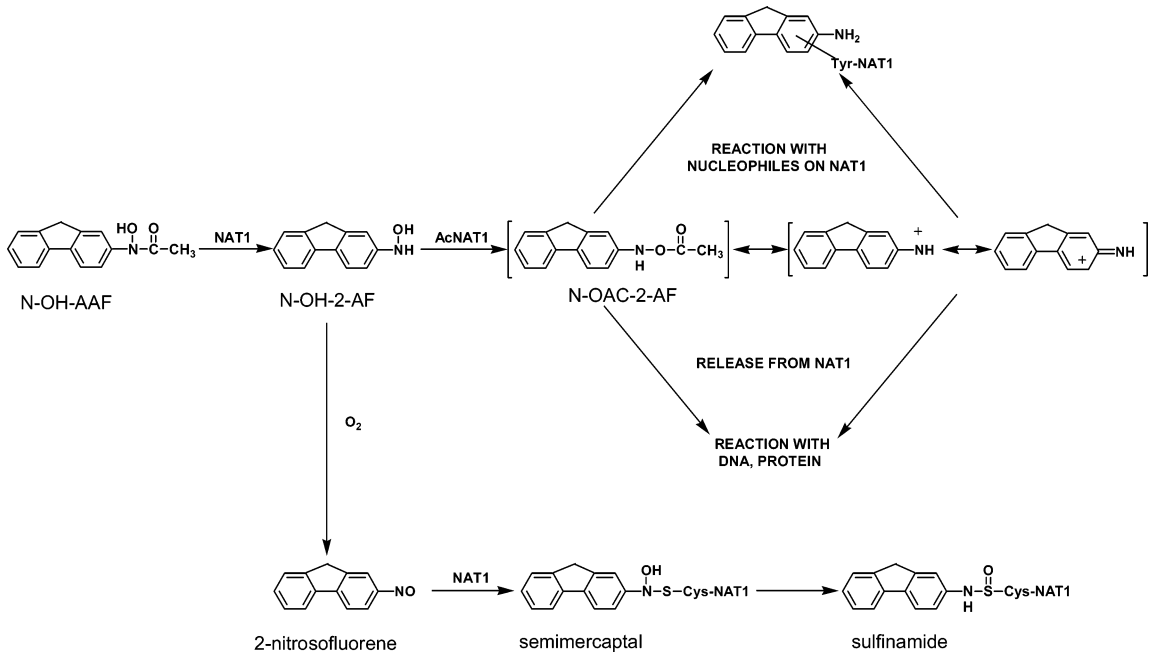

(Scheme 1). Reaction of 2-nitrosofluorene with Cys68 would proceed through the intermediate semimercaptal to the sulfinamide by a mechanism that has been well-characterized (*26*). Although most N-arylhydroxylamines undergo facile oxidative conversion to arylnitroso compounds, the specific mechanism responsible for oxidation of N-OH-AF in the present experiments is unknown. Appropriate precautions were taken to ensure that the substrate, N-OH-AAF, did not contain trace amounts of 2-nitrosofluorene and that buffers were free of metals that could catalyze oxidation of N-OH-AF.

The role of nitrosoarenes in protein adduct formation has received attention principally in the development of biomarkers for molecular dosimetry. After exposure to arylamines, N-arylhydroxylamines are formed metabolically and are further oxidized in erythrocytes to nitrosoarenes, which form sulfinamide adducts with hemoglobin. After collection of the hemoglobin and hydrolysis of the sulfinamide adducts, the arylamines are quantitated to estimate the extent of exposure (*37*, *38*). X-ray crystallographic analysis was used to identify Cys93β as the hemoglobin residue modified by the 4-nitrosobiphenyl metabolite of N-hydroxy-4-aminobiphenyl (*39*). The analytical approach described herein offers the possibility of identifying specific sulfinamide adducted residues by using MALDI Q-TOF tandem mass spectrometry to detect sulfinic acid modifications. These results also indicate that since NAT1 is expressed in most human tissues (*40*), NAT1-catalyzed hydrolysis of N-arylhydroxamic acids may serve as a specific source of exposure of various target tissues to N-arylhydroxylamines and nitrosoarenes. In this regard, it is well-established that N-arylhydroxamic acids are in vivo metabolites of a variety of arylamines, arylamides, and nitroarenes (*41*, *42*). Thus, NAT1, as well as the less substrate specific microsomal carboxylesterases, may contribute to the hydrolytic disposition of N-arylhydroxamic acids (*43*).

We reported earlier that glutathione, in a concentration 200-fold greater than that of N-OH-AAF, had a modest effect on the N-OH-AAF-mediated inactivation of NAT1, whereas an identical concentration of cysteine afforded complete protection of the enzyme from inactivation (*19*). Similar results were obtained in the present study in which a 10-fold greater concentration of N-OH-AAF was incubated with a 20-fold greater concentration of NAT1 in the presence of the same concentration of glutathione or cysteine (10 mM) used in the previous experiments. The inability of glutathione to attenuate the formation of the Cys68 (2-fluorenyl)sulfinamide adduct seems inconsistent with its well-documented propensity for reacting with arylnitroso compounds in the absence of catalysis by glutathione S-transferases (*26*, *27*, *32*). Cysteine, with a molecular weight of approximately 40% of that of glutathione, largely prevented the formation of the Cys68 adduct with NAT1 and prevented most of the loss of enzyme activity. The greater effectiveness of cysteine may be due in part to its slightly lower pK_a (8.15) relative to that of glutathione (8.56), which results in 15% of cysteine existing as the nucleophilic thiolate ion at pH 7.4, as compared to approximately 6.5% of glutathione. The smaller molecular dimensions of cysteine also may contribute to its ability to protect the active site thiolate of NAT1. In related experiments, a 10-fold excess of 2-nitrosofluorene caused a complete loss of NAT1 activity within 30 s. GSH had no effect on NAT1 inactivation by 2-nitrosofluorene, but the presence of cysteine in the incubation mixture prevented most of the loss of activity (data not shown). The latter results are consistent with those obtained with GSH and cysteine when NAT1 was treated with N-OH-AAF.

Most research on the bioactivation of N-arylhydroxamic acids and arylhydroxylamines by NATs has focused on the formation of N-acetoxyarylamines, such as N-OAc-AF (Scheme 1), which undergo solvolytic decomposition to form highly electrophilic arylnitrenium ions (*14*, *25*, *44*−*46*). Bioactivation of N-OH-AAF by NAT1 resulted in the production of only minor NAT1 adducts, which might be attributed to reaction of amino acids with an arylnitrenium ion. Tyr186, which is conserved in human NAT1 and in hamster, rat, and mouse NAT1 and NAT2, was modified by 2-AF, as was Tyr17, which is not present

in hamster NAT2 or in human, rat, and mouse NATs (*47*, *48*). The specific structures of the 2-AF−tyrosine adducts, which were formed in very small quantities, have not been elucidated. On the basis of mechanistic considerations, it is likely that either the 1-position or the 3-position of 2-AF is bonded to the tyrosine residues, although bond formation between tyrosine and the amino group of 2-AF is also possible. NAT-catalyzed bioactivation of N-OH-AAF in the presence of methionine yields exclusively 1- and 3-methylmercapto-2-AF (*11*, *44*).

The characterization of arylamine−protein adducts has received considerably less attention than structural analysis of arylamine−DNA adducts (*3*). Chemical studies on liver protein from rats fed N-methyl-4-aminoazobenzene revealed that the major adducts included 3-(homocystein-S-yl)-N-methyl-4-aminoazobenzene, a product of reaction with methionine, and two tyrosine adducts (*5*). The proposed structures of the tyrosine adducts were N-(3-tyrosyl)-N-methyl-4-aminoazobenzene and 3-(3-tyrosyl)-N-methyl-4-aminoazobenzene. Thus, both of the latter modifications appeared to involve covalent bond formation at the 3-position of tyrosine, ortho to the 4-hydroxyl group. Such 3-tyrosyl adduct formation would also be feasible for reaction between an electrophilic 2-AF metabolite and the tyrosine residues in NAT1. Coles et al. identified alcohol dehydrogenase as a specific protein target in the liver of rats fed N,N-dimethyl-4-aminoazobenzene and demonstrated unequivocally that the adducted residue was Met306, in which a covalent bond had formed between the sulfur atom of methionine and the 3-position of the carcinogen (*49*). Also, a 3-tryptophanyl-4-acetylaminobiphenyl adduct at Trp214 was identified in serum albumin of rats that had been administered 4-aminobiphenyl (*50*).

This study demonstrates that 2-nitrosofluorene, generated in the course of bioactivation of N-OH-AAF by NAT1, is responsible for the irreversible inactivation of NAT1. Thus, an enzyme inactivation that appeared to be consistent, at least kinetically, with a mechanism-based process, may be more accurately described as a metabolic inactivation (*51*). The toxicological implications of the covalent modification and inactivation of NAT1 by nitrosoarenes are unknown. Butcher et al. reported that incubation of human peripheral blood mononuclear cells with either N-hydroxy-*p*-aminobenzoic acid or N-hydroxysulfamethoxazole causes irreversible inactivation of NAT1; it was suggested that the nitroso compounds are the ultimate inactivating agents (*52*). Protein conjugates formed by nitroso metabolites of the antibacterial sulfonamides have been implicated in the etiology of their immunotoxic and cytotoxic effects, but little information is available regarding specific sites of modification on protein targets (*53*, *54*). The experimental approach employed in the present research may be of utility in the identification of cysteine residues modified by nitrososulfonamides and other nitrosoarenes.

Acknowledgment. We thank Drs. Thomas Krick, LeeAnn Higgins, and Sudha Marimanikkuppam of the Mass Spectrometry Consortium for the Life Sciences, University of Minnesota, for their advice and assistance. This research was supported in part by U.S. Public Health Service Grant CA55334 from the National Cancer Institute and by a Development Grant in Drug Design from the Department of Medicinal Chemistry, University of Minnesota.

References

(1) Kriek, E. (1992) Fifty years of research on N-acetyl-2-aminofluorene, one of the most versatile compounds in experimental cancer research. *Cancer Res. Clin. Oncol. 118*, 481−489.

(2) Miller, J. A. (1998) The metabolism of xenobiotics to reactive electrophiles in chemical carcinogenesis and mutagenesis: a collaboration with Elizabeth Cavert Miller and our associates. *Drug Metab. Rev. 30*, 645−674.

(3) Beland, F. A., and Kadlubar, F. F. (1990) Metabolic activation and DNA adducts of aromatic amines and nitroaromatic hydrocarbons. *Handbook Exp. Pharmacol. 94/I*, 267−325.

(4) Hanna, P. E. (1996) Metabolic activation and detoxification of arylamines. *Curr. Med. Chem. 3*, 195−210.

(5) Lin, J. K., Miller, J. A., and Miller, E. C. (1969) Studies on structures of polar dyes derived from the liver proteins of rats fed N-methyl-4-aminoazobenzene. III. Tyrosine and homocysteine sulfoxide polar dyes. *Biochemistry 8*, 1573−1582.

(6) Barry, E. J., Malejka-Giganti, D., and Gutmann, H. R. (1969/70) Interaction of aromatic amines with rat liver proteins in vivo. III. On the mechanism of binding of the carcinogens, N-2-fluorenylacetamide and N-hydroxy-2-fluorenylacetamide, to the soluble proteins. *Chem.-Biol. Interact. 1*, 139−155.

(7) Hanna, P. E. (1994) N-acetyltransferases, O-acetyltransferases and N,O-acetyltransferases: enzymology and bioactivation. *Adv. Pharmacol. 27*, 401−430.

(8) Hein, D. W., Doll, M. A., Fretland, A. J., Leff, M. A., Webb, S. J., Xiao, G. H., Devanaboyina, U.-S., Nangju, N. A., and Feng, Y. (2000) Molecular genetics and epidemiology of the NAT1 and NAT2 acetylation polymorphisms. *Cancer Epidemiol. Biomarkers Prev. 9*, 29−42.

(9) Banks, R. B., and Hanna, P. E. (1979) Arylhydroxamic acid N,O-acyltransferase. Apparent suicide inactivation by carcinogenic N-arylhydroxamic acids. *Biochem. Biophys. Res. Comm. 91*, 1423−1429.

(10) Wick, M. J., and Hanna, P. E. (1990) Bioactivation of N-arylhydroxamic acids by rat hepatic N-acetyltransferase. Detection of multiple enzyme forms by mechanism based inactivation. *Biochem. Pharmacol. 39*, 991−1003.

(11) Bartsch, H., Dworkin, M., Miller, J. A., and Miller, E. C. (1972) Electrophilic N-acetoxyaminoarenes derived from carcinogenic N-hydroxy-N-acetylaminofluorenes by enzymatic deacetylation and transacetylation in liver. *Biochim. Biophys. Acta 286*, 272−298.

(12) King, C. M. (1974) Mechanism of reaction, tissue distribution, and inhibition of arylhydroxamic acid acyltransferase. *Cancer Res. 34*, 1503−1515.

(13) Hanna, P. E., Banks, R. B., and Marhevka, V. C. (1982) Suicide inactivation of hamster hepatic arylhydroxamic acid N,O-acyltransferase. A selective probe of N-acetyltransferase multiplicity. *Mol. Pharmacol. 21*, 159−165.

(14) Marhevka, V. C., Ebner, N. A., Sehon, R. D., and Hanna, P. E. (1985) Mechanism-based inactivation of N-arylhydroxamic acid N,O-acyltransferase by 7-substituted-N-hydroxy-2-acetamidofluorenes. *J. Med. Chem. 28*, 18−24.

(15) Mangold, B. L. K., and Hanna, P. E. (1982) Arylhydroxamic acid N,O-acyltransferase substrates. Acetyl transfer and electrophile generating activity of N-hydroxy-N-(4-alkyl, 4-alkenyl, and 4-cyclohexylphenyl)acetamides. *J. Med. Chem. 25*, 630−638.

(16) Hanna, P. E., El-Ghandour, A. M., and McCormack, M. E. (1990) Analogues of N-hydroxy-4-acetylaminobiphenyl as substrates and inactivators of hamster hepatic acetyltransferases. *Xenobiotica 20*, 739−751.

(17) Smith, T. J., and Hanna, P. E. (1988) Hepatic N-acetyltransferases: selective inactivation in vivo by a carcinogenic N-arylhydroxamic acid. *Biochem. Pharmacol. 37*, 427−434.

(18) Sticha, K. R. K., Sieg, C. A., Bergstrom, C. P., Hanna, P. E., and Wagner, C. R. (1997) Overexpression and large scale purification of recombinant hamster polymorphic arylamine N-acetyltransferase as a dihydrofolate reductase fusion protein. *Protein Expression Purif. 10*, 141−153.

(19) Sticha, K. R. K., Bergstrom, C. P., Wagner, C. R., and Hanna, P. E. (1998) Characterization of hamster recombinant monomorphic and polymorphic arylamine N-acetyltransferases. Bioactivation and mechanism based inactivation studies with N-hydroxy-2-acetylaminofluorene. *Biochem. Pharmacol. 56*, 47−59.

(20) *NIH Guidelines for the Laboratory Use of Chemical Carcinogens* (1981) NIH Publication No. 81-2385, U.S. Government Printing Office, Washington, DC.

(21) Westra, J. G. (1981) A rapid and simple synthesis of reactive metabolites of carcinogenic aromatic amines in high yield. *Carcinogenesis 2*, 355−357.

(22) Bradford, M. M. (1976) A rapid and sensitive method for the quantitation of microgram quantities of protein utilizing the principle of protein-dye binding. *Anal. Biochem. 72*, 248−254.
(23) Lotlikar, P. D., Miller, E. C., Miller, J. A., and Margreth, A. (1965) The enzymatic reduction of the N-hydroxy derivatives of 2-acetylaminofluorene and related carcinogens by tissue preparations. *Cancer Res. 25*, 1743−1752.
(24) Bergstrom, C. P., Wagner, C. R., Ann, D. K., and Hanna, P. E. (1995) Hamster monomorphic arylamine N-acetyltransferase: Expression in *Escherichia coli* and purification. *Protein Expression Purif. 6*, 45−55.
(25) Kadlubar, F. F., and Beland, F. A. (1985) Chemical properties of ultimate carcinogenic metabolites of arylamines and arylamides. In *Polycylic Hydrocarbons and Carcinogenesis*, ACS Symposium Series No. 283 (Harvey, R. G., Ed.) pp 341−370, American Chemical Society, Washington, DC.
(26) Kazanis, S., and McClelland, R. A. (1992) Electrophilic intermediate in the reaction of glutathione and nitrosoarenes. *J. Am. Chem. Soc. 114*, 3052−3059.
(27) Mulder, G. J., Unruh, L. E., Evans, F. E., Ketterer, B., and Kadlubar, F. F. (1982) Formation and identification of glutathione conjugates from 2-nitrosofluorene and N-hydroxy-2-aminofluorene. *Chem.-Biol. Interact. 39*, 111−127.
(28) Turesky, R. J., Skipper, P. L., and Tannenbaum, S. R. (1987) Binding of 2-amino-3-methylimidazo[4,5-f]quinoline to hemoglobin and albumin in vivo in the rat. Identification of an adduct suitable for dosimetry. *Carcinogenesis 8*, 1537−1542.
(29) Johnson, R. S., Martin, S. A., and Biemann, K. (1988) Collision-induced fragmentation of $(M+H)^+$ ions of peptides. Side chain specific sequence ions. *Int. J. Mass Spectrom. Ion Processes 86*, 137−154.
(30) Hein, D. W., Doll, M. A., Fretland, A. J., Gray, K., Deitz, A. C., Feng, Y., Jiang, W., Rustan, T. D., Satran, S. L., and Wilkie, T. R., Sr. (1997) Rodent models of the human acetylation polymorphism. *Mutat. Res. 376*, 101−106.
(31) Hein, D. W., Doll, M. A., Rustan, T. D., Gray, K., Feng, Y., Ferguson, R. J., and Grant, D. M. (1993) Metabolic activation and deactivation of arylamine carcinogens by recombinant human NAT1 and polymorphic NAT2 acetyltransferases. *Carcinogenesis 14*, 1633−1638.
(32) Eyer, P. (1979) Reactions of nitrosobenzene with reduced glutathione. *Chem.-Biol. Interact. 24*, 227−239.
(33) Dolle, B., Topner, W., and Neumann, H. G. (1980) Reaction of arylnitroso compounds with mercaptans. *Xenobiotica 10*, 527−536.
(34) Payton, M., Mushtaq, A., Yu, T.-W., Wu, L.-J., Sinclair, J., and Sim, E. (2001) Eubacterial arylamine N-acetyltransferases-identification and comparison of 18 members of the protein family with conserved active site cysteine, histidine and aspartate residues. *Microbiology 147*, 1137−1147.
(35) Dupret, J.-M., and Grant, D. M. (1992) Site-directed mutagenesis of recombinant human arylamine N-acetyltransferase expressed in *Escherichia coli*. *J. Biol. Chem. 267*, 7381−7385.
(36) Novak, M., and Rajagopal, S. (2002) Correlations of nitrenium ion selectivities with quantitative mutagenicity and carcinogenicity of the corresponding amines. *Chem. Res. Toxicol. 15*, 1495−1503.
(37) Skipper, P. L., Peng, X., Soohoo, C. K., and Tannenbaum, S. R. (1994) Protein adducts as biomarkers of human carcinogen exposure. *Drug Metab. Rev. 26*, 111−124.
(38) Skipper, P. L., and Tannenbaum, S. R. (1990) Protein adducts in the molecular dosimetry of chemical carcinogens. *Carcinogenesis 11*, 507−518.
(39) Ringe, D., Turesky, R. J., Skipper, P. L., and Tannenbaum, S. R. (1988) Structure of the single stable hemoglobin adduct formed by 4-aminobiphenyl in vivo. *Chem. Res. Toxicol. 1*, 22−24.
(40) Rodrigues-Lima, F., Cooper, R. N., Goudeau, B., Atmane, N., Chamagne, A.-M., Butler-Browne, G., Sim, E., Vicart, P., and Dupret, J.-M. (2003) Skeletal muscles express the xenobiotic-metabolizing enzyme arylamine N-acetyltransferase. *J. Histochem. Cytochem. 51*, 789−796.
(41) Weisburger, J. H., and Weisburger, E. K. (1973) Biochemical formation and pharmacological, toxicological, and pathological properties of hydroxylamines and hydroxamic acids. *Pharmacol. Rev. 25*, 1−66.
(42) Moller, L., Rafter, J., and Gustafsson, J.-A. (1987) Metabolism of the carcinogenic air pollutant 2-nitrofluorene in the rat. *Carcinogenesis 8*, 637−645.
(43) Wang, C. Y. (1994) Microsomal amidases and carboxylesterases. In *Conjugation−Deconjugation Reactions in Drug Metabolism and Toxicity* (Kauffman, F. C., Ed.) pp 161−187, Springer-Verlag, New York.
(44) Elfarra, A., and Hanna, P. E. (1985) Substituent effects on the bioactivation of 2-(N-hydroxyacetamido)fluorenes by N-arylhydroxamic acid N,O-acyltransferase. *J. Med. Chem. 28*, 1453−1460.
(45) Boteju, L., and Hanna, P. E. (1994) Arylamine-nucleoside adduct formation: evidance for arylnitrene involvement in the reactions of an N-acetoxyarylamine. *Chem. Res. Toxicol. 7*, 684−689.
(46) Kennedy, S. A., Novak, M., and Kolb, B. A. (1997) Reactions of ester derivatives of carcinogenic N-(4-biphenylyl)hydroxylamine and the corresponding hydroxamic acid with purine nucleosides. *J. Am. Chem. Soc. 119*, 7654−7664.
(47) Payton, M., Auty, R., Delgoda, R., Everett, M., and Sim, E. (1999) Cloning and characterization of arylamine N-acetyltransferse genes from *Mycobacterium smegmatis* and *Mycobacterium tuberculosis*: increased expression results in isoniazid resistance. *J. Bacteriol. 181*, 1343−1347.
(48) Doll, M. A., and Hein, D. W. (1995) Cloning, sequencing and expression of NAT1 and NAT2 encoding genes from rapid and slow acetylator inbred rats. *Pharmacogenetics 5*, 247−251.
(49) Coles, B., Beale, D., Miller, D., Lay, J., Kadlubar, F., Aitkens, A., and Ketterer, B. (1987) The binding of an aminoazo dye carcinogen to a specific methionine residue in rat liver alcohol dehydrogenase in vivo. *Chem.-Biol. Interact. 64*, 181−192.
(50) Skipper, P. L., Obiedzinski, M. W., Tannenbaum, S. R., Miller, D. W., Mitchum, R. K., and Kadlubar, F. F. (1985) Identification of the major serum albumin adduct formed by 4-aminobiphenyl in vivo in rats. *Cancer Res. 45*, 5122−5127.
(51) Silverman, R. B. (1988) *Mechanism-Based Enzyme Inactivation: Chemistry and Enzymology*, Vol. I, pp 3−30, CRC Press, Boca Raton, FL.
(52) Butcher, N. J., Ilett, K. F., and Minchin, R. F. (2000) Inactivation of human arylamine N-acetyltransferase 1 by the hydroxylamine of p-aminobenzoic acid. *Biochem. Pharmacol. 60*, 1829−1836.
(53) Summan, M., and Cribb, A. E. (2002) Novel nonlabile covalent binding of sulfamethoxazole reactive metabolites to cultured human lymphoid cells. *Chem.-Biol. Interact. 142*, 155−173.
(54) Naisbitt, D. J., Farrell, J., Gordon, S. F., Maggs, J. L., Burkhart, C., Pichler, W. J., Pirmohamed, M., and Park, K. B. (2002) Covalent binding of the nitroso metabolite of sulfamethoxazole leads to toxicity and major histocompatibility complex-restricted antigen presentation. *Mol. Pharmacol. 62*, 628−637.

TX030045O